

We are IntechOpen, the world's leading publisher of Open Access books Built by scientists, for scientists

6,900

Open access books available

186,000

International authors and editors

200M

Downloads

Our authors are among the

154

Countries delivered to

TOP 1%

most cited scientists

12.2%

Contributors from top 500 universities



WEB OF SCIENCE™

Selection of our books indexed in the Book Citation Index
in Web of Science™ Core Collection (BKCI)

Interested in publishing with us?
Contact book.department@intechopen.com

Numbers displayed above are based on latest data collected.
For more information visit www.intechopen.com



Sorel Cements from Tunisian Natural Brines

Halim Hammi, Amal Brichni, Salima Aggoun and
Adel Mnif

Additional information is available at the end of the chapter

<http://dx.doi.org/10.5772/intechopen.74315>

Abstract

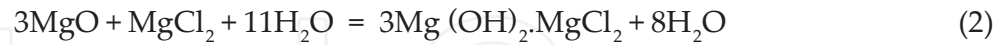
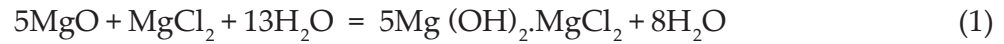
In this chapter, the experimental design methodology is applied to optimize the formation conditions of magnesium chloride cement. A factorial design to model and to optimize the operating parameters that govern the formation was used. The studied factors were mass ratio of $\text{MgCl}_2 \cdot 6\text{H}_2\text{O}/\text{MgO}$, mixing time and stirring speed. The considered responses were compressive strength and setting time. The optimum operating conditions were quite efficient to have a good compressive strength and suitable setting time. The phases' compositions of the magnesium oxychloride cement were evaluated by X-ray diffraction, the morphological properties were examined by scanning electron microscopy (SEM) method and their thermal behavior was analyzed by differential thermal analysis/thermogravimetric analysis (DTA/TGA). The raw materials used in the study were magnesium oxide and magnesium chloride hexahydrate obtained from natural brines in the south of Tunisia.

Keywords: magnesium oxychloride cement, experimental design methodology, optimization

1. Introduction

Magnesium chloride cement (MOC) has superior properties as compared to ordinary Portland cement such as high compressive strength [1], good resistance to abrasion, rapid hardening rate, good cohesiveness and high fire resistance [2], and it can be used with all kinds of aggregates [3]. The main used applications are architectural applications such as the construction of industrial floors, construction of thermal and acoustical insulating panels [4] and other prefabricated building boards [5]. The basic chemical reaction system of the MOC system is $\text{MgO}-\text{MgCl}_2-\text{H}_2\text{O}$ [6, 7]. The main bonding phases found in hardened MOC is $5\text{Mg}(\text{OH})_2$.

$\text{MgCl}_2 \cdot 8\text{H}_2\text{O}$ (phase 5) and $3\text{Mg}(\text{OH})_2 \cdot \text{MgCl}_2 \cdot 8\text{H}_2\text{O}$ (phase 3) which are obtained by the following chemical reactions [7]:



They are the only stable phases in the system $\text{MgO-MgCl}_2\text{-H}_2\text{O}$. Due to the presence of excess water, a parallel or competitive reaction, corresponding to magnesium oxide hydration, can take place:



The presence of $\text{Mg}(\text{OH})_2$ indicates the low quality of magnesium oxychloride cement.

Furthermore, the widespread use of magnesium oxychloride cement has been limited because of loss of strength on prolonged excessive exposure to water [8]. Much research has long been processed to improve the water resistance of magnesium oxychloride based on the ability to it binding to various organic and inorganic aggregates such as high active SiO_2 [9, 10], active aluminates [11] sulfates and phosphoric acid or phosphate [12].

In this chapter, the influence of three factors (mass ratio of MgCl_2/MgO , mixing time and stirring speed) on compressive strength and setting time of MOC was carried out. The application of the experimental design methodology was used in order to maximize synthesis yield by searching for optimum experimental conditions in a less number of experiments.

2. Raw materials from natural brines

The Tunisian territory contains a great number of sebkhas and chotts, especially in the South. The more important ones are Chott El Jerid, Sebkha El Melah of Zarzis, Sebkha Oum el Khialate, Sebkha El Briga and Sebkha El Adhibate (**Figure 1**) [13]. Previous geological, hydrogeological and geochemical studies proved that these deposits contain considerable reserves of natural brines (**Table 1**).

The meteorological conditions in the South of Tunisia and particularly at Sebkha El Melah of Zarzis (**Figure 2**) are favorable for the recovery of the existing salts by solar evaporation. The raw material is taken from Aïn Serab, located at the Northern border of Sebkha El Melah of Zarzis. This choice is justified by the advantages present in this mineral resource and the influence on the economic sector for possible industrial exploitation [14].

These salt lakes which are considered as important material resources useful for industry and agriculture. They are called sebkha or chott, and they cover a large part of Tunisian land. The liquid raw material enclosed in these deposits is named brine and always assimilated to the quinary system: Na^+ , K^+ , $\text{Mg}^{2+}/\text{Cl}^-$, $\text{SO}_4^{2-}/\text{H}_2\text{O}$. These solutions are valuable and expected to play an important role in the economic sector. To take advantage of this raw material, several works

Sites	Geographic location	Surface, km ²	Total reserves, 10 ⁶ m ³	Recoverable reserves, 10 ⁶ m ³	Total salinity, g/L
Chott Jerid	Tozeur	5000	5000	600	330
S. El Melah	Zarzis	150	600	160	335
S. oum El Khialate	Tataouine	75	50	17	150
S. El Adhibate	Tunisian Libyan border	125	245	100	260
S. El Briga	Tunisian Libyan border	22	78	18	330

Table 1. Characteristics of south Tunisian sebkhas and chotts.

2.1. Magnesium oxide

Exceptional proprieties of MgO as a catalytic material [15, 16] or as an additive in building supplies (Sorel cement, lightweight building panels) and superconductor products have attracted both fundamental and application studies [17–22].

Magnesium oxide (MgO or periclase) is one among the most industrially important magnesium compounds. Approximately 20% of worldwide production came from seawater, brines and desalination reject brine [15]. Magnesium oxide is used as an exceptionally important material in catalysis [15, 16], toxic waste remediation [18] or as additives in refractories, paints, in the manufacture of fertilizers, animal feedstuffs, building materials (Sorel cement, lightweight building panels) and superconductor products [19–21]. A panel of fundamental and applied studies is encountered in literature [21–25]. It shows particularly that magnesium hydroxide production from seawater or brine precipitates by adding a strong base and after separation is calcined to produce MgO. Furthermore, magnesia qualities may differ depending upon the physicochemical conditions of preparation and the precursor type.

In the literature, MgO was prepared mainly by calcination of Mg(OH)₂ obtained either by precipitation [21, 22] or by MgO hydration [21, 23–25]. In our case, magnesium oxide was produced from magnesium sulfate (MgSO₄·7H₂O) by precipitation into Mg(OH)₂ using a strong base (NH₄OH) in the first step and then calcined in a programmable furnace under controllable conditions to produce MgO in the second step.

The sensitivity of the present reactions to several parameters was carried out. These considerations altogether led to applying the experimental design methodology in order to maximize synthesis yield by searching for the optimum experimental conditions in a smaller number of experiments.

2.2. Magnesium chloride

Magnesium chloride is industrially useful in some agricultural applications. It is mainly used for magnesium metal production and Sorel cement manufacturing (Büchel et al., 2000). Frequently, natural raw material is complex and must be treated to recover solid magnesium chloride. Various procedures (Boyum et al., 1973; Burke and Smith, 1949; Fezei et al., 2009; Smith, 1970) have been developed in order to produce this salt from natural brines. The



Figure 2. Sebkhia El Melah of Zarzis [14].

present work is devoted to magnesium chloride hexahydrate recovery from a mixed salt solution. 1,4-Dioxan was chosen to achieve this aim. The action of this organic solvent on magnesium chloride has been often studied in the case of pure magnesium chloride solutions (Gaska, 1967; Weissenberg, 1969).

As shown in **Figure 3**, the investigated process is mainly composed of six stages. The adopted flow sheet is principally supported by the previous works on natural brines (Janeček, 1907; Berthon, 1962; Cohen-Adad et al., 2002; M'nif and Rokbani, 2004; Hammi, 2004) usually described using the oceanic quinary diagram Na^+ , K^+ , $\text{Mg}^{2+}/\text{Cl}^-$, $\text{SO}_4^{2-}/\text{H}_2\text{O}$. This useful graphic-tool is helpful in natural brines exploitation or valorization. In fact, it defines, during the system's evolution, the number, the nature, the composition and the relative quantity of different condensed phases that crystallize or disappear. The first treatment step consists in evaporating at 35°C the raw brine to precipitate the maximum of sodium chloride (halite).

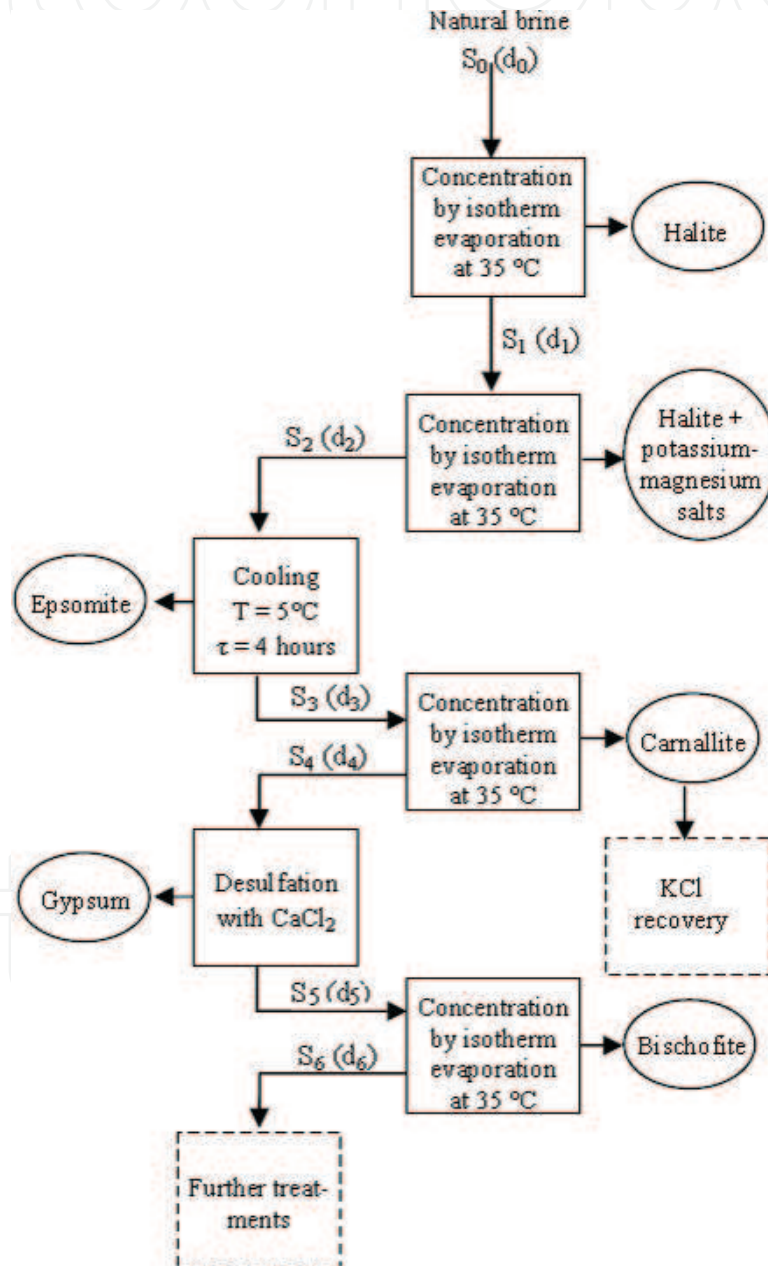


Figure 3. Flow sheet of the process for the bischofite salt recovery from Sebkhia El Melah natural brine.

In the second step, The precipitated salts consist of sodium chloride and small amounts of magnesium-potassium double salt. The third stage consists in maintaining the obtained magnesium salts saturated solution under stirring during four hours at 5°C and to recover the precipitated salt. The fourth step consists in precipitating the potassium- magnesium double salt, carnallite ($\text{KCl} \cdot \text{MgCl}_2 \cdot 6\text{H}_2\text{O}$) to eliminate potassium ions; in order to avoid interference with the production of an end product having good quality. In the two last stages of the process the solution is desulphated by reaction with calcium chloride solution. After removing the calcium sulfate precipitate, the resulting brine; consisted of magnesium chloride together with residual potassium and sodium chloride; is concentrated by evaporation at 35°C to precipitate the magnesium chloride salt.

3. Results and discussion

3.1. Experimental procedure

Magnesium oxide powder was mixed with magnesium chloride solution mechanically to form homogenous MOC pastes. The weight of MgO is fixed and the weight of $\text{MgCl}_2 \cdot 6\text{H}_2\text{O}$ has been varied. Mixtures were cast in cylindrical molds (26 mm in diameter, 50 mm high) and stored for 24 h, then unmolded and air-cured for 28 days.

The X-ray diffraction (XRD) analysis was carried out on the powdered sample using X-ray powder diffractometer (XRD PHILIPS) with Cu K radiation ($\lambda \text{K} = 1.54 \text{ \AA}$).

Differential thermograms were obtained using the Netzsch 449 STA F1 Jupiter thermal analysis system. The rate of heating was 15°C/min.

The microstructure of the samples was examined using scanning electron microscope, the Carl ZEISS LEICA S430i model.

Measurement of thermal conductivity was performed in dry state using the photothermal deflection technique. Setting time was determined by using the Vicat Apparatus.

Porosity accessible to water of MOC is determined according to EN 12390-7 norm. The measurement of porosity in water under a vacuum of 0.1 bar quantifies the volume of open pores (accessible to water) using the following protocol:

Cement samples are placed in sealed desiccators and kept under vacuum of 0.1 bar for 12 h.

Previously degassed water is introduced progressively in desiccators to fill all the pores of samples, without introducing air bubbles.

Once the samples are saturated, they are kept immersed in water for 24 h, and finally we determined hydrostatic mass $m_{\text{ss}}^{\text{imm}}$ and saturated dry surface mass m_{ss} .

The porosity is calculated by Eq. (4):

$$\frac{m_{sss} - m_{dry}}{m_{sss} - m_{sss}^{imm}} \quad (4)$$

where

m_{sss} : the saturated dry surface mass of the sample;

m_{dry} : the mass of sample before saturation; and.

m_{sss}^{imm} : mass of sample measured in water.

3.2. Studied factors and experimental domains

According to the preparation of MOC, three quantitative factors are chosen: mass ratio of $MgCl_2/MgO$, stirring speed and mixing time. The corresponding variables and their levels (set according to the data of preliminary experiments and the equipment abilities) are given in **Table 2**. The two experimental responses tracked were compressive strength (Y_1) and the setting time (Y_2).

To test the direct influence of the three studied factors as well as their possible interaction effects on the measured experimental responses, we have realized a two-level complete factorial design 2^3 which is expected to provide excellent information concerning not only the main effects but also the double interaction effects.

The experimental design and the measured responses are summarized in **Table 2**.

Comparing MOC and Portland cement (setting time between 2 and 3 h), it is found that MOC has a faster setting. It also has better mechanical strength.

For a very short setting time (6 min), MOC has a high strength (75.48 MPa): in this case the cement is recommended for applications that require fast setting (decoration use, restoration of monuments, damaged marble, etc.).

For a longer setting time (64 min), it has a good mechanical strength (46.59 MPa): in this case the cement is recommended for applications which require a longer setting time (floor covering).

Considering that the interaction effects between three or more factors are negligible, the factor effect estimation is computed by Mathieu et al. [26]; according to Goupy [27]:

$$b_i = \frac{\sum_j^N \pm Y_j}{N} \quad (5)$$

where b_i is the effect estimation of the factor i , Y_j is the response j , and N is the number of experiences.

The pooled variance estimation used to determine the significant factors is computed as

$$S_a^2 = \frac{\sum_i^n v_i S_i^2}{n} \quad (6)$$

No. exp.	Mass ratio of MgCl ₂ / MgO	Mixing time (min)	Stirring speed (rpm)	Compressive strength (MPa)	Setting time (min)
1	1.42	5	650	49.47	20
2	2.22	5	650	46.59	64
3	1.42	15	650	4.55	17
4	2.22	15	650	21.20	37
5	1.42	5	1600	41.38	14
6	2.22	5	1600	76.40	41
7	1.42	15	1600	75.48	6
8	2.22	15	1600	20.50	32
9	1.82	10	1125	67.00	30
10	1.82	10	1125	60.54	31
11	1.82	10	1125	59.00	28

Table 2. Factorial matrix 2³.

where s_a^2 is the pooled experimental variance, s_i^2 is the experimental variance estimation i , v_i is the degree of freedom i , and $n = \sum v_i$ is the degree of freedom of the pooled experimental variance.

4. Identification of the influential factors

Based on check student for an error risk $\alpha = 5\%$, it was found that tabulated = 4.303. **Table 3** summarizes the factor effects estimation for the two responses: compressive strength (Y_1) and setting time (Y_2).

Coefficient	Y_1				Y_2			
	Value	SD	t.exp	P	Value	SD	t.exp	P
b0	47.464	1.279	37.087	0.000726	29.090	0.460	63.1634	0.000251
b1	-0.773	1.500	-0.515	0.657478	14.625	0.540	27.0802	0.001361
b2	-11.513	1.500	7.672	0.016568	-5.875	0.540	-10.878	0.008345
b3	11.493	1.500	7.658	0.016624	-5.625	0.540	-10.415	0.009093
b12	-8.808	1.500	-5.869	0.027819	-3.125	0.540	-5.7864	0.028592
b13	-4.216	1.500	-2.809	0.106780	-1.375	0.540	-2.5460	0.125809
b23	6.063	1.500	4.040	0.056143	1.625	0.540	3.0089	0.094979
b123	-13.691	1.500	-9.123	0.011802	2.875	0.540	5.3235	0.033522

Table 3. Factor signification for the two responses Y_1 and Y_2 .

The two models are represented by the equations given below:

Compressive strength:

$$Y_{cal_1} = 47.464 - 11.513X_2 + 11.493X_3 - 8.808X_1X_2 - 13.6913X_1X_2X_3 \quad (7)$$

Setting time:

$$Y_{cal_2} = 29.090 + 14.625X_1 - 5.875X_2 - 5.625X_3 - 3.125X_1X_2 + 2.875X_1X_2X_3 \quad (8)$$

4.1. Analysis of residue

Figure 4 reveals the distribution of the calculated values versus experimental values for the two responses (Y_1 and Y_2). The points are almost randomly distributed about the line representing exact agreement, providing good agreements between experimental values and those calculated using the model.

4.2. Analysis of variance

Table 4 summarizes the variance analysis of the chosen responses Y_1 and Y_2 .

The main results for Y_1 and Y_2 are, respectively, 333.601 and 12.539, as lack of fit mean squares and 18.017 and 2.333 as the estimation of experimental variance. Thus, the values of the ratio between the lack of fit mean square and the estimation of experimental variance 18.51568 and 5.3739 for the responses Y_1 and Y_2 are inferior to tabled $F_{4,2}^{0.05}$ and $F_{3,2}^{0.05}$, respectively. Consequently, it is possible to confirm the validity of the two elaborated models. In addition, the ratios between the regression mean square and the residual mean square for the three responses Y_1 and Y_2 (4.638 and 5.3739) are superior to the tabled $F_{4,6}^{0.05}$ and $F_{5,5}^{0.05}$, respectively. Thus, the significant variables, applied to elaborate the three models, have a large significance on their responses.

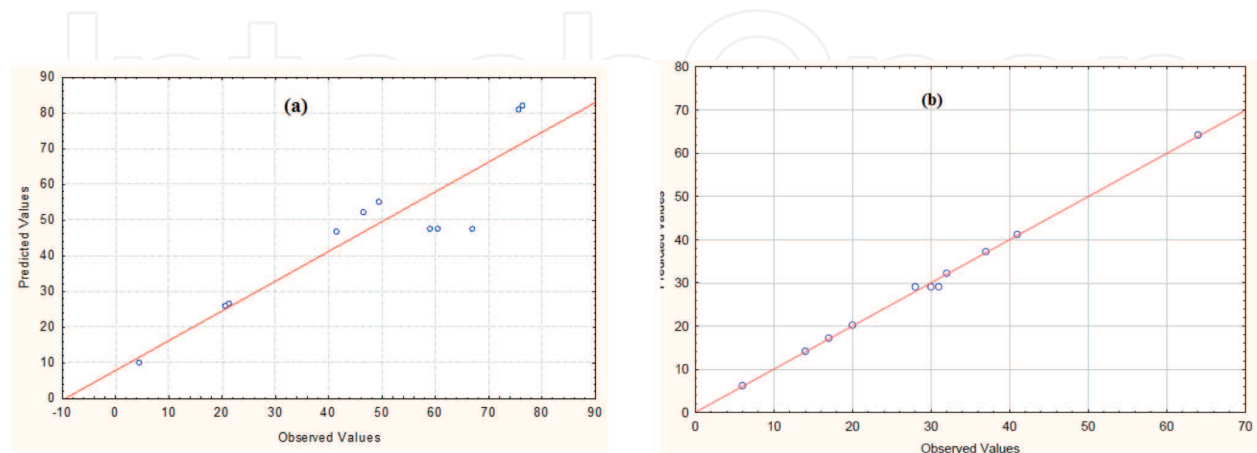


Figure 4. Calculated versus experimental values graph (a) for compressive strength (b) for setting time.

Source of variation	SS	DF	MS	Ratio	P
Compressive strength					
Regression	4237.738	4	1059.4345	4.63837	0.048
Residual	1370.437	6	228.40616		
Lack of fit	1334.403	4	333.601	18.51568	0.051897
Pure error	36,034	2	18.017		
Total	5608.174	10	1059.4345		
Setting time					
Regression	2384.625	5	476.925	56.40478	0.0000
Residual	42.277	5	8.4554		
Lack of fit	37.610	3	12.539	5.3739	0.160892
Pure error	4.667	2	2.333		
Total	2426.909	10	476.925		

Table 4. Analysis of variance.

4.2.1. Optimization

For selecting the optimal conditions we try to strike a compromise between the two responses to have good compressive strength and a suitable setting time.

By merely regarding values and signs of these significant effects, we conclude that maximization of the two responses is reached for experience number 6 (compressive strength = 76.40 MPa and setting time = 41 min):

Mass ratio of $MgCl_2 \cdot 6H_2O/MgO$ (X_1): 2.22

Mixing time (X_2): 5 min

Stirring speed (X_3): 1125 rpm

The phase diagram of the ternary MOC system ($MgO-MgCl_2-H_2O$) [5] at an ambient temperature is illustrated in **Figure 5** with the composition point of the optimum which is located near phase 5 responsible for good compressive strength of the cement.

4.3. Characterization

Figure 6 shows the XRD pattern of MOC with an optimal condition. It can be found that phase 5 is present. This phase is the major product responsible for hardening and the strength of MOC. We measured porosity accessible to water, we found that the total porosity of MOC is 4% which is in good accordance with other results in literature [28].

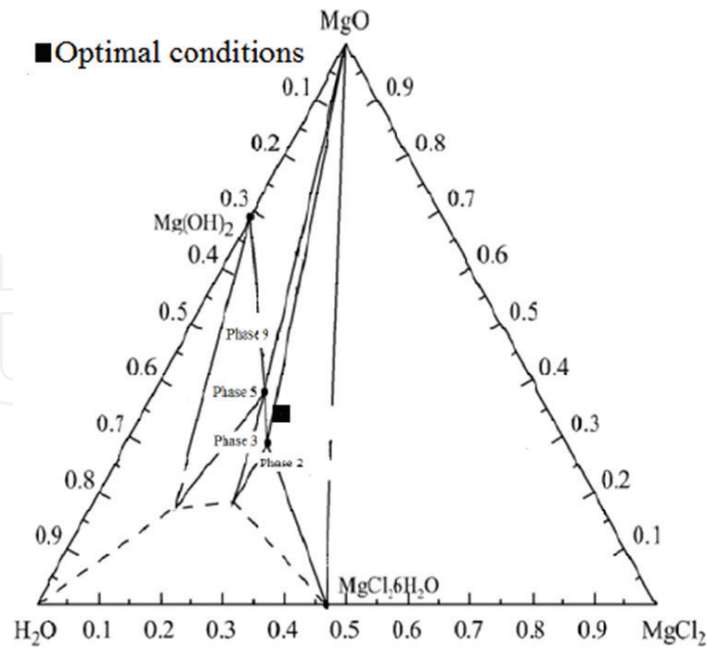


Figure 5. Phase diagram of the ternary MOC system [5].

The thermal conductivity of cement is 0.8 w/mK. The morphology of MOC is shown in Figure 7. We can see a rough surface with a dense network of needle-like crystals of 500 nm which has a high strength (phase 5). Thermal analysis of MOC is shown in Figure 8. Six endothermic events appear on the DTA curves of MOC during heating. Thermal decomposition requires a dehydration stage of the crystalline phase 5 $\text{Mg(OH)}_2\text{MgCl}_2\cdot 8\text{H}_2\text{O}$ at 179°C to obtain anhydrous materials.

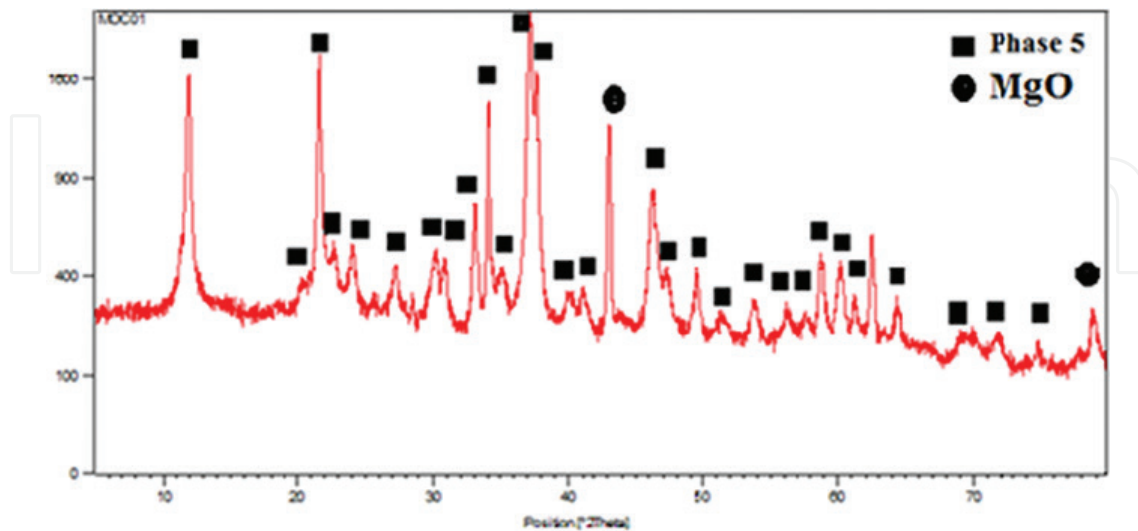


Figure 6. XRD patterns of MOC.

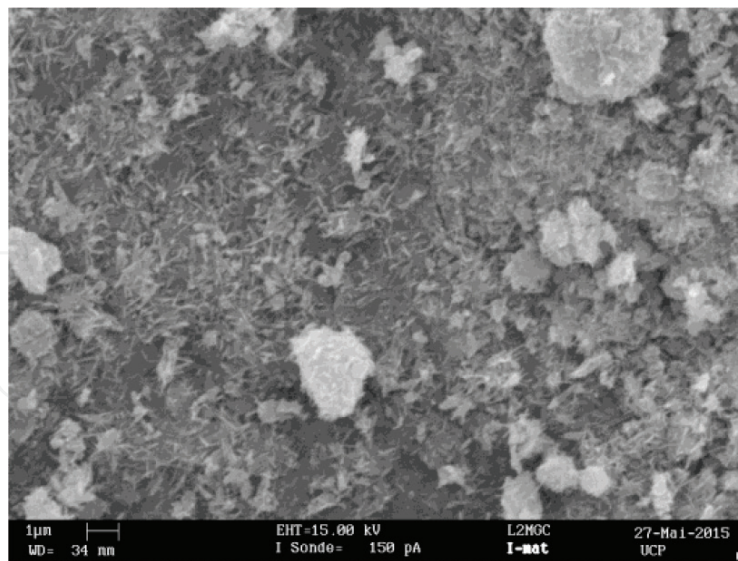


Figure 7. SEM analysis of MOC.

The other deflections in this curve at 358, 414, 484, and 711°C present the decomposition stage of $5 \text{Mg}(\text{OH})_2 \cdot \text{MgCl}_2$ and the loss of MgCl_2 . The last deflection at 1100°C represents the decomposition to obtain the final solid product MgO .

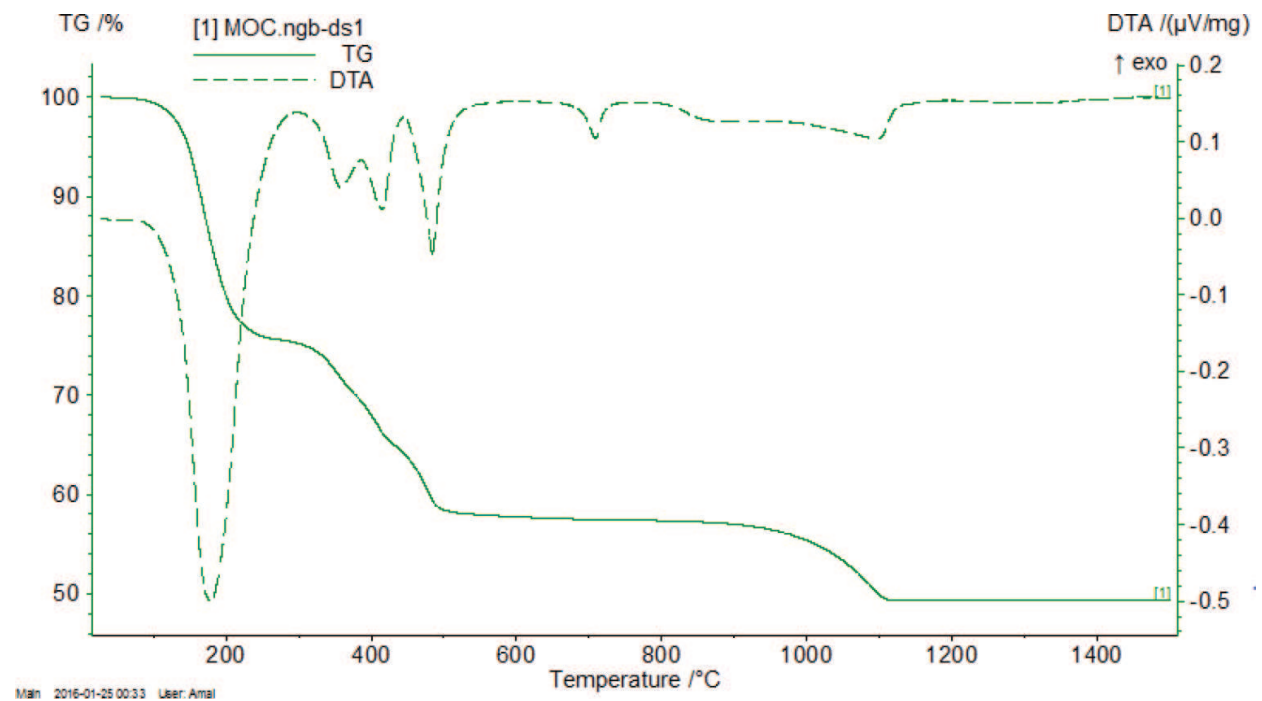


Figure 8. TG and DTA curves of MOC.

5. Conclusion

The formation of MOC from natural brines was carried out in this study using experimental design. The results showed that there is an agreement between the experimental values and those calculated from the model developed which confirms its validity. The optimal conditions are $\text{MgCl}_2 \cdot 6\text{H}_2\text{O}/\text{MgO}$ (X1): 2.22, mixing time (X2): 5 min and stirring speed (X3): 1125 rpm. The responses are compressive strength = 76.40 MPa and setting time = 41 min. The interpretation of results found by DRX, IR, SEM and TG-DTA confirms the presence of phase 5 which is responsible for the good compressive strength of magnesium oxychloride cement.

Acknowledgements

This chapter was supported by a grant from Ministry of Higher Scientific Research of Tunisia. The authors would like to thank the technical team of the National Research Centre of Materials Sciences in Borj Cedria Technological Park and of L2MGC in the University of Cergy-Pontoise.

Author details

Halim Hammi^{1*}, Amal Bricni^{1,2}, Salima Aggoun³ and Adel Mnif¹

*Address all correspondence to: halimhammi2015@gmail.com

1 Useful Material Valorization Laboratory, National Center for Research in Materials Sciences, Soliman, Tunisia

2 Université de Tunis El Manar, Faculté des Sciences de Tunis, Tunis, Tunisie

3 University of Cergy-Pontoise (L2MGC), Neuville Sur Oise, Cergy-Pontoise Cedex, France

References

- [1] Li J, Yu Y, Li G. The influence of compound additive on magnesium oxychloride cement/urban refuse floor tile. *Construction and Building Materials*. 2008;**22**:521-525
- [2] Montle JF, Mayhan KG. The role of magnesium oxychloride as a fireresistive material. *Fire Technology*. 1974;**10**:201-210
- [3] Siddique R, Naik TR. Naik, Properties of concrete containing scrap-tire rubber-an overview. *Waste Management*. 2004;**24**:563-569
- [4] Yu H. *Magnesium Oxychloride Cement and Its Application*. 1st ed. Beijing: China Building Materials Industry Press; 1993

- [5] Zongjini L, Chau CK. Influence of molar ratios on properties of magnesium oxychloride cement. *Cement and Concrete Research*. 2007;**37**:866-870
- [6] Deng DH, Zhang CM. The formation mechanism of the hydrate phases in magnesium oxychloride cement. *Cement and Concrete Research*. 1999;**29**(9):1365-1371
- [7] Li Y, Yu HF, Dong JM, Wen J, S Y. Reseach Development on Hydration Product, Phase Transformation and Water Resistance Evaluation Method of Magnesium Oxychloride Cement. *Journal of the Chinese Ceramic Society*. 2013;**41**:1465-1473
- [8] Beaudoin JJ, Ramachandran VS. Strength development in Magnesium Oxychloride and Other Cement and Concrete Research. 1975;**5**:617-630
- [9] Wu CY, Zhang HF, Yu HF. The effects of aluminum-leached coal fly ash residue on magnesium oxychloride cement. *Advances in Cement Research*. 2013;**25**:254-261
- [10] Xu K, Guo Y, Sun Q, Dong S, Li Z. Research on Chemical Intermediates. 2012;**39**:1417-1428
- [11] Deng DH, Zhang CM. The effect of aluminate minerals on the phases in magnesiumoxychloride cement. *Cement and Concrete Research*. 1996;**26**:1203-1211
- [12] Li Y, Yu H, Zheng L, Wen J, Wu C, Tan Y. Compressive strength of fly ash magnesium oxychloride cement containing granite wastes. *Construction and Building Materials*. 2013;**38**:1-7
- [13] M'nif A. Valorisation des saumures du sud tunisien, Habilitation. Fac. Sc. Tunis; 2001
- [14] Perthuisot JP, La Sebka El Melah de Zarzis: Genèse et Évolution d'un Bassin Paralique, École normale supérieure, Paris 1975
- [15] Büchel KH, Moretto H-H, Woditch P. *Industrial Inorganic Chemistry*. Weinheim: Wiley-Vch, Verlag GmbH; 2000:235
- [16] Liang SHC, Gay ID. A ¹³C solid-state NMR study of the chemisorption and decomposition of ethanol on MgO. *Journal of Catalysis*. 1986;**101**:293
- [17] Tsuji H, Yagi F, Hattori H, Kita H. Preparation of nanometer magnesia with high surface area and study on the influencing factors of the preparation process. *Journal of Catalysis*. 1994;**148**:759
- [18] Copp AN. Magnesia/magnesite. *American Ceramic Society Bulletin*. 1995;**74**:135
- [19] Wang W, Qiao X, Chen J. The role of acetic acid in magnesium oxide preparation via chemical precipitation. *Journal of the American Ceramic Society*. 2008;**91**:1697-1699
- [20] Yuan YS, Wong MS, Wang SS. Mechanical behavior of MgO-whisker reinforced (Bi, Pb)₂Sr₂Ca₂Cu₃O_y high-temperature superconducting composite. *Journal of Materials Research*. 1996;**11**:8
- [21] Yang PD, Lieber C. Nanorod-superconductor composites: A pathway to materials with high critical current densities. *Science*. 1996;**273**:1836

- [22] Wagner GW, Bartram PW, Koper O, Klabunde KJ. Reactions of VX, GD, and HD with nanosize MgO. *The Journal of Physical Chemistry. B.* 1999;**103**:3225
- [23] Boldyrev AI, Simons J. Polyhedral ionic molecules. *Journal of the American Chemical Society.* 1997;**119**(20):4618-4621
- [24] Zhou M, Zhu H, Jiao Y, Rao Y, Hark S, Liu Y, Peng L, Li Q. Optical and electrical properties of Ga-doped ZnO nanowire arrays on conducting substrates. *Journal of Physical Chemistry C.* 2009;**113**(20):8945-8947
- [25] Sterrer M, Diwald O, Knozinger E. Vacancies and electron deficient surface anions on the surface of MgO nanoparticles. *The Journal of Physical Chemistry. B.* 2000;**104**:3601
- [26] Mathieu D, Phan Tan Luu R. Nemrod-W Software. France: Aix-Marseille III University; 1999
- [27] Goupy J. Modélisation par les plans d'expériences, *Techniques de l'ingénieur. Traité Mesures et Contrôle.* R 275. CFC. Paris. 2000. pp. 1-23
- [28] Zhao S, Fan J, Sun W. Utilization of Iron Ore Tailings as Fine Aggregate in Ultra-High Performance Concrete. *Construction and Building Materials.* 2014;**50**:540-548